DRAFT

SAND96-2272C

SAND--96-2272C

VSHOT: A Tool for Characterizing Large, Imprecise Reflectors

Scott A. Jones, Daniel R. Neal, James K. Gruetzner, Richard M. Houser, Robert M. Edgar

Sandia National Laboratories
Albuquerque, New Mexico

Timothy J. Wendelin

National Renewable Energy Laboratories
Golden, Colorado

CONF-960848--29

RECEIVED

SEP 19 1996

OSTI

ABSTRACT

A prototype Video Scanning Hartmann Optical Tester (VSHOT) has been developed to characterize the optics of dish-type solar concentrators. VSHOT is a flexible platform that may characterize any large reflector with a focal length over diameter ratio (f/#) greater than 0.45, and RMS optical error in the 0.1-10 milliradian range. The VSHOT hardware, software, and operation are described. Measurement uncertainty and preliminary test results are discussed. Another potential application being explored for the VSHOT is the quality assurance of slumped-glass automobile windshields. Preliminary test results from a reference optic and a section of a windshield are presented.

Keywords: solar concentrators, Hartmann testing, laser applications, optical testing, sheet glass testing

1. INTRODUCTION

The scanning Hartmann approach was selected from a number of candidate methods for use in the original Scanning Hartmann Optical Test (SHOT) system because it was well suited to characterizing the variety of large dish concentrators being developed in the Department of Energy's Solar Thermal Technology Program[1] that have RMS slope errors of 0.5-3 milliradians (mrad). In addition to being versatile and appropriate for slope errors in the 0.1-10 mrad range, this approach was selected because it was based on direct measurement of slope and provided a quantitative map of optical errors. Multiple step (scanning) operation was preferred over a single pass Hartmann because the deep paraboloids and large optical errors of solar concentrators would lead to overlap of return spots. Also, the large and varied shapes of concentrators developed would each require an expensive mask to be constructed. Likewise, interferometric methods were inappropriate for the slope error regime required because interference fringes would be too closely spaced and difficult to analyze[1]. Results from actual, on-sun testing and a more qualitative tool called the $2f$ test[2,3] closely agree with the original SHOT results[4], supporting the usefulness of the scanning Hartmann approach in general, and the original device's accuracy as a test device in specific.

2. DESCRIPTION

The Video Scanning Hartmann Optical Test (VSHOT) is an evolutionary step beyond the original SHOT system. It utilizes a video system to measure return spot locations, providing higher speed testing and requiring less operator oversight. An optical scanner with a larger cone angle (60°) permits testing of a dish concentrator with a smaller focal length over diameter ratio (f/#) or an entire, multi-faceted dish. A smaller and lower power (class IIIa) laser is also used, enhancing worker safety. Utilization of a higher speed computer has allowed software to be re-written to expand capabilities and greatly improve the user interface. All of these improvements have yielded a faster, safer, more robust test platform with capability

MASTER

1

DISCLAIMER

DISCLAIMER

not only as a laboratory test instrument, but also as a manufacturing quality assurance tool and field test device. The application of VSHOT capabilities to other solar and non-solar applications is possible.

A schematic of the VSHOT is shown in Figure 1. The prototype system consists of a 133-MHz Pentium® computer, 16-bit X/Y scanners with a 60° optical cone angle, a 24 channel digital I/O board, an 8-bit CCD camera, a video digitizing and processing card, a class IIIa He-Ne laser, and miscellaneous hardware and cabling. The X/Y scanners and laser together constitute what will be termed in this paper the laser scanner, or just scanner. Software coding is mostly in VisualBasic®, with some subroutines written in C++ and dynamically linked at run time.
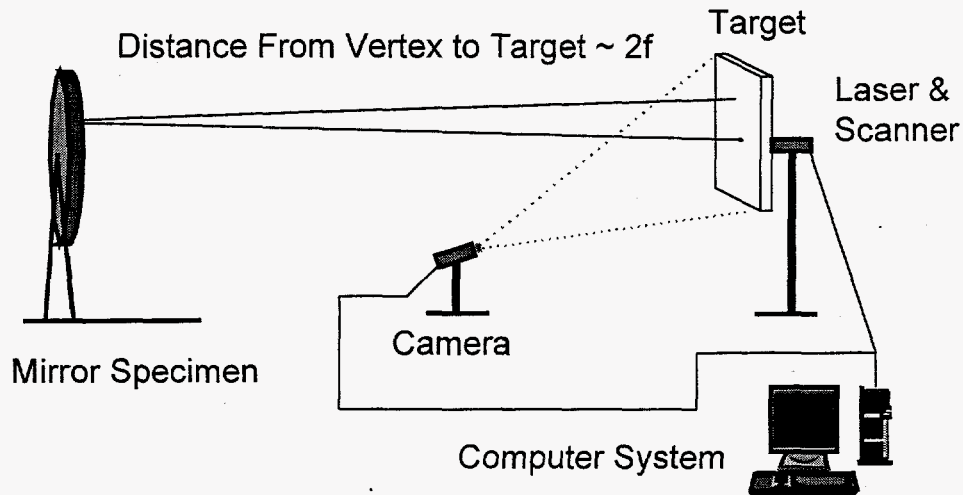
Figure 1. Schematic of the VSHOT

A test is performed by placing the reflective article at roughly twice its focal length from the scanner, so that the return spots land on the target. The laser is steered by the scanner mirrors to hit the test article. The location of the return spot is measured with the CCD camera and video board. This process is repeated across the surface of the test article in a user-defined test pattern. From the scanner aiming angles and return spot locations, the slope at each point and the shape of the mirror's surface are computed using the coordinate definitions in Figures 2a and 2b.

Figure 2a. VSHOT coordinates in 3-Dimensions

Figure 2b. VSHOT coordinates in 2-Dimensions
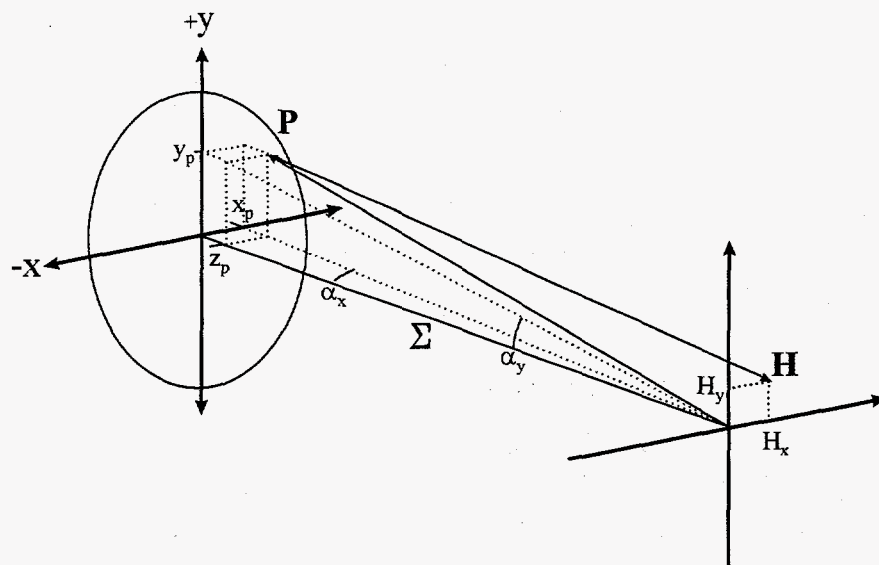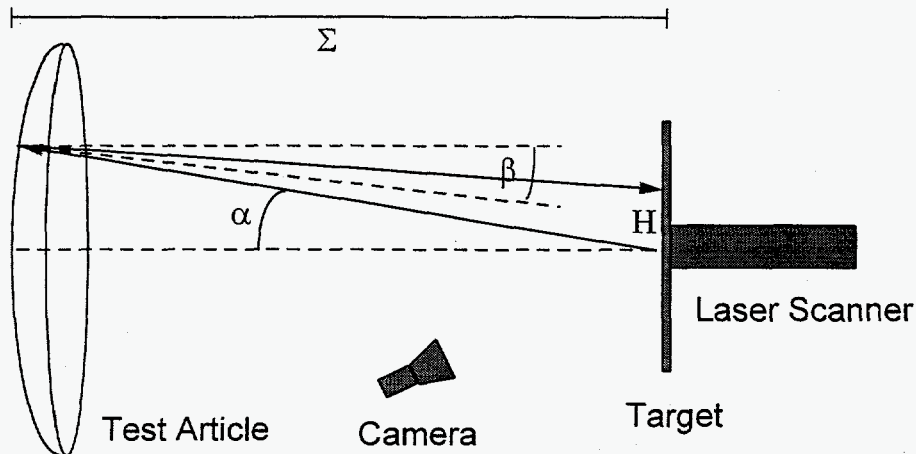
3. CALIBRATION

It is essential to calibrate both the video and laser scanner subsystems before performing tests. The maximum accuracy of the VSHOT is bounded by the accuracy of the subsystem calibrations that calculate the pointing angles of the scanner and the location of the return spot.

3.1 Video Calibration

The video system calibration creates a "map" of the target surface that relates linear distances on the target to camera coordinates (pixels). The calibration takes about 2 minutes time. A video calibration is normally performed just prior to a test, after the test article and the target have been properly aligned. In addition, the video system must be calibrated anytime the target is moved or the camera view is adjusted.
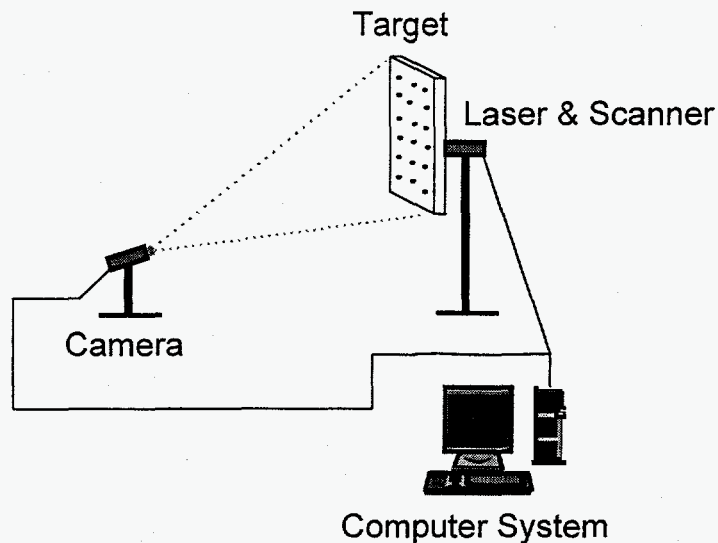

Figure 3. Schematic of test set-up during video system calibration

For the calibration, a rectangular grid of spots with known spacing is temporarily mounted on the target and the camera is positioned to view the required target area as shown in Figure 3. The centroids of each

circular spot are determined to a fraction of a pixel, and a fit of the surface to equation (1) is performed knowing the actual grid spacing in both X and Y directions. The temporary spot grid is removed and work continues.

$$z(x, y) = \sum_{i=0}^{k} \sum_{j=0}^{i} B_{i,j}(x)^{j}(y)^{i-j} \tag{1}$$

In this equation, B is the fit parameter, and x and y are the system coordinates. The surface is described by z. Currently, a fourth-order ($k=4$) equation is used. This effectively corrects for off-axis positioning of the camera as well as optical errors such as pincushion. Further details on the selection of the equation and the fitting process may be found in section 5 (Data Analysis).

3.2 Laser Scanner Calibration

The laser scanner calibration "map" relates true pointing angles to scanner coordinates (scanner steps). A calibration must be performed only when the orientation between the laser and scanner mirrors changes (normally a rare event) or if the required cone angle for testing exceeds the calibration regime. A scanner calibration target must be of a sufficient size and distance for the desired cone angle of calibration and carefully aligned orthogonally and centered facing the laser scanner. Figure 4 shows the equipment setup for laser calibration.
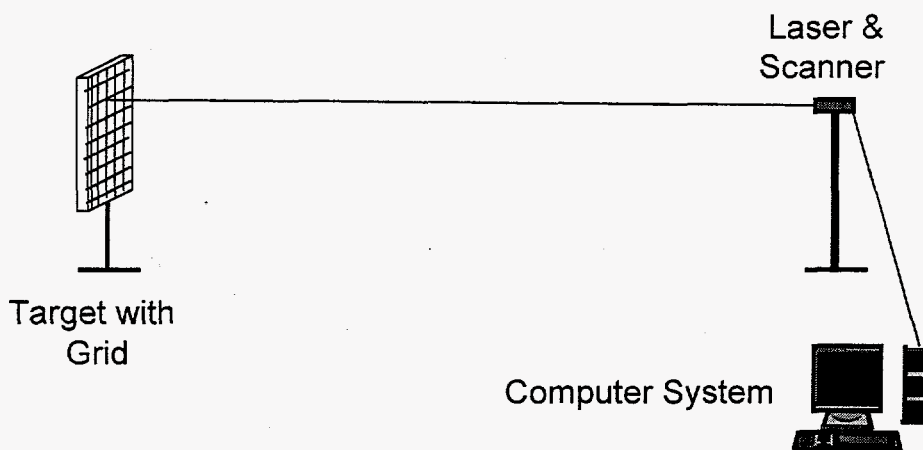
Figure 4. Equipment set-up for laser calibration.

A special large target imprinted with gridlines in needed for the laser calibration. The target size and distance from the scanner is selected to accommodate the desired scanner cone angle. The operator controls the scanner position. Scanner positions required to make the beam land centered upon each grid intersection are recorded. This is performed several times, with the positions averaged due to the uncertainty in visually aligning the laser spot with the grid intersections. The averaged scanner coordinates and location of each grid intersection are then fit with equation (1) for each X and Y axis scanner mirror to complete the mapping process. This approach to laser scanner calibration is tedious, lengthy (~15 hours), and may require two personnel—one to adjust the scanner position at the computer, and the other to carefully watch the movement of the beam on the target. However, it provides a direct map from pointing angles to scanner steps. Another system that utilizes the video system and promises to be much faster is under development.

3.3 Calibration Errors

The video and scanner calibrations are subject to alignment errors and measurement uncertainties, a subject discussed in greater depth later. Nonetheless, it is worthwhile to briefly discuss this topic here as it relates to calibration. The scanner calibration assumes the target is centered and orthogonal to the axis of the laser scanner. Any departure from this introduces bias error into the calibration. A gunsight-like system is used to insure the target is centered on the optical axis of the scanner, and the four corner of the target are made equidistant from the scanner origin to insure the target is orthogonal.

Error in the measurement of the distance between the scanner mirrors and the target is another possible source of calibration error. Consequently, it is preferable to use as large a target as possible so it may be positioned farther away and the relative uncertainty in distance reduced. If the grid of spots used in the video calibration is displaced from the center of the target or rotated from the scanner X/Y axes, a bias error would be introduced into the video calibration, as will be seen later.

4. TEST EXECUTION

First the geometry of the test article is defined. Then a test pattern is defined to fill that geometry with the desired number of points. The user may select a standard rectangular test pattern, or opt to randomize this slightly. Randomization of the test pattern is intended to improve the measurement of surface features with a similar scale to the grid spacing.

Next the test article must be positioned at roughly twice its focal length and aligned. Unlike spherical mirrors, parabolic mirrors have a range of focal lengths and radii of curvature. The smallest return spot pattern may be achieved by positioning the mirror somewhere between the shortest (saggital) and longest (tangential) radius of curvature. The VSHOT software permits the user to continuously draw the test pattern, or other shapes, on the test article to assist with positioning and alignment by determining the size and location of the return spot pattern. Once the test article is positioned, the distance Σ is measured carefully.

Then the video system is positioned, typically off-axis, and adjused for the correct zoom and focus. Background, threshold, and source spot blockout features are adjusted to insure high quality results. The video system is calibrated, the calibration grid is removed, and the image features are readjusted for testing. A test description may be entered into the computer system for record keeping. At this point, testing commences.

The operator may initially want to monitor the test to insure proper operation, but this is not required as the system is fully automated. Optional diagnostics display the video image, centroid location, test pattern, and return spot pattern. Any rays that miss the target, return directly to the source hole, or have intensities less than a specified threshold may be revisited by the operator at the end of the test to determine the cause of the "miss." The prototype system requires about 2.5 seconds per test point with all system diagnostics turned on. We anticipate reducing that by a factor of 10 with planned improvements.

After all the test points have been measured, the raw data (scanner steps and video pixels) are unmapped using the scanner and video calibrations to true coordinates (scanner angles α_x and α_y, and return spot location H_x and H_y). This unmapped data, descriptions of the article geometry and test setup, and video calibration data are saved in a file for later use.

5. DATA ANALYSIS

Data analysis occurs separately from testing, permitting multiple fits from one set of unmapped test data. A surface fit is performed to raw slope data, inherently providing better accuracy than fitting to surface measurements and deriving slopes. The two variable polynomial introduced in equation 1 was chosen for

the surface fit because key optical parameters have simple relations to the polynomial coefficients[5]. A Zernike polynomial was not used because it is in polar coordinates, unlike all the raw test data that are in Cartesian coordinates.

Since the optical axis of the test article may not be perfectly aligned with the scanner axis, we modify equation (1) to permit x- and y-axis offsets:

$$z(x - \Delta x, y - \Delta y) = \sum_{i=0}^{k} \sum_{j=0}^{i} B_{i,j}(x - \Delta x)^{j}(y - \Delta y)^{i-j} \qquad (2)$$

The VSHOT measures slopes, so we wish to fit to the partial derivatives of the surface equation:

$$\frac{dz}{d(x - \Delta x)} = \sum_{i=0}^{k-1} \sum_{j=0}^{i} D_{i,j}(x - \Delta x)^{j}(y - \Delta y)^{i-j} \qquad (3)$$

and

$$\frac{dz}{d(y - \Delta y)} = \sum_{i=0}^{k-1} \sum_{j=0}^{i} E_{i,j}(x - \Delta x)^{j}(y - \Delta y)^{i-j} \qquad (4)$$

Where,

$$B_{i,j} = \frac{D_{i-1,j-1}}{j} \qquad (5)$$

and

$$B_{i,j} = \frac{E_{i-1,j}}{i-j} \qquad (6)$$

The fitting of the test data to a surface is an iterative process. A perfect parabolic surface shape with user specified focal length is assumed for the first iteration, and point P is defined as the intersection of the outgoing laser beam with this surface. Then the return beam vector is found from the locations of P and H. The slope at point P, β, is found from the law of reflection knowing the outgoing and return beam vectors. β is then reduced to its x and y components for fitting. This is done for every test point measured.

The β_x slopes are fit to equation (3) using a standard least squares approach, and the surface coefficients are found from equation (5). Then the β_y slopes are fit to equation (4), and the surface coefficients found from (6). Note that this duplicates the calculation of some $B_{i,j}$ surface coefficients. Since there is always some noise in the data, different results may found for these coefficients in each fit direction so they are averaged:

$$B_{i,j} = \frac{1}{2}\left(\frac{D_{i-1,j-1}}{j} + \frac{E_{i-1,j}}{i-j}\right) \qquad (7)$$

Given this new fit of the mirror surface, every test point P is again located, and new β_x and β_y slopes are calculated. A least squares fit is performed again. The residuals (slope errors at each point) are recorded and a RMS value calculated. This process is repeated until convergence occurs. Convergence is considered achieved when the change in RMS slope error between consecutive runs is less than a threshold value. We have used threshold values of 0.005, which typically require 3-5 iterations to achieve.

In solar applications, the ideal shape is parabolic, so the RMS error from a 2nd order fit may be treated as a measure of the optical quality of the test article, assuming the residuals are random in nature. In general, higher order fits are necessary to reduce the residuals to truly random uncertainty. These higher order fits contain all asymmetric surface properties and best describe the mathematical surface. The 2nd order fits are most useful however because vector plots of the residual slopes immediately reveal departures from the ideal shape and thus provide information on how to correct them.

When the fit is complete, optical parameters may be determined from the function coefficients. Of greatest interest is the focal length of the test article. Since asymmetry is accounted for in the fit, independent foci may be found in each Cartesian direction. These focal lengths are given by:

$$f_x = \frac{1}{4B_{2,2}} \tag{8}$$

$$f_y = \frac{1}{4B_{2,0}} \tag{9}$$

It is important to note that the aforementioned analysis assumes a constant laser beam source location. In reality, the apparent source of the laser beam shifts as the scanner mirrors turn. This becomes significant for small f/# and large cone angle tests. There are two ways to address this issue. The first is to physically correct for this movement using a two lens array that re-images the source at the target plane. The laser calibration procedure would correct for lens aberrations. This approach was used in the original SHOT and is also desirable because a smaller hole in the target is thus required. The second approach is to use software to correct for the movement of this source. A determination of which method will be used has not yet been made.

6. MEASUREMENT UNCERTAINTY

In this section we discuss an analytical estimate of the VSHOT measurement uncertainty. This is very valuable because it illustrates the nature of the error sources, determine the dominant contributors, and identify areas for improvement. Also very valuable is an experimental test of measurement precision and accuracy through a sensitivity study. Such a study was performed on the original SHOT[6], and is planned for the VSHOT.

There are two error classes which must be considered. One is bias or fixed error and the other is precision or random error. Bias error for the VSHOT is difficult to assess in the development stages. Although assumed to be small relative to the random error, it can enter into the system uncertainty through the calibration of the video camera and laser scanner. Determination of the bias error will be accomplished as part of the experimental program. For now, the bias error will be ignored and this analysis will focus on estimating the precision error.

The VSHOT ultimately determines β_x and β_y, the slope of the surface at the intersection point. For simplicity, we will discuss uncertainty in just one dimension, as shown in Figure 2a.

Three errors can occur in the determination of β: the measurements of Σ, α and H. These parameters are interrelated and errors in one or more of these parameters can have cascading effects on the others. Because a closed form solution of the overall error contribution is complicated, a numerical approach was used to assess the sensitivity of the measurement system to errors in these three quantities. A spreadsheet program was developed which calculates the sensitivity of the angle β to small errors in Σ, H and α. This sensitivity is also dependent on dish size and focal length. For a given f/#, the quantities $d\beta/d\Sigma$, $d\beta/d\alpha$ an $d\beta/dH_x$ are generated as a function of dish radius. The maximum total precision error is calculated as the root-sum-square of the maximum of each of these three parameters over the dish radius.

Six uncertainty case studies are listed in Table 1. Cases 1 and 2 represent the uncertainty estimate for the bench scale reference test described in the next section. The error contributions (dΣ, dα, dH) were determined as follows. For long Σ range values, it was assumed that Σ can be measured to within $\pm$ 0.5 centimeters. For shorter Σ range values it was assumed that measurements can be made to within $\pm$ 1.0 millimeter. The resolution of the camera used to develop the VSHOT is 649 pixels in the horizontal direction by 245 pixels in the vertical direction. The size of the return target is 1 meter by 1 meter. Centroids of images can be calculated to within 1/100 of a pixel. Using the vertical direction then as the limiting case, this translates into an uncertainty in H of 4.1×10^{-6} meters. The laser scanner is capable of repeatable measurements of angle α to within 2.5×10^{-5} radians.

Table 1. VSHOT measurement uncertainty case study

	Dish Diameter (m)	F/D	Focal Length (m)	Σ (m)	dΣ (m)	dα (rads)	dH (m)	Total Error (mrads)
Case 1	0.1	3.0	0.3	0.6	0.000	2.5E-5	4.1E-6	0.002
Case 2	0.1	3.0	0.3	0.6	0.002	2.5E-5	4.1E-6	0.136
Case 3	1.0	0.4	0.4	0.8	0.001	2.5E-5	4.1E-6	0.175
Case 4	1.0	3.0	3..0	6.0	0.005	2.5E-5	4.1E-6	0.035
Case 5	3.0	3.0	9.0	18.0	0.005	2.5E-5	4.1E-6	0.011
Case 6	15.0	0.4	6.0	12.0	0.005	2.5E-5	4.1E-6	0.055
Case 7	15.0	0.4	6.0	12.0	0.010	2.5E-5	4.1E-6	0.111

The results show that over a wide range of dish sizes and focal lengths, the maximum precision error expected in the measurement of surface slope would be < 0.2 milliradians. The measurement of β is also shown to be most sensitive to errors in Σ. However, as focal length increases (and therefore Σ) the sensitivity to errors in Σ decreases.. Most solar thermal concentrator optics fall into the 3.0 to 15.0 meter diameter range and so the expected precision error would fall to < 0.05 milliradians. This precision error is more than acceptable for characterizing solar thermal concentrator optics where acceptable departures from ideal surface slope are in the range of 0.5 to 3.0 milliradians. Thus the VSHOT is a sufficiently accurate tool for characterizing solar thermal concentrator optics. It should also be noted that all these cases were run for a centroid location accuracy of 1/1000 of a pixel (or twice that shown in the table) with no change in the total error to the accuracy displayed in Table 1. Thus the video capture error is not a significant contributor to the total error.

7. PRELIMINARY RESULTS

7.1 Test of a Reference Optic

The first preliminary test performed was on a high quality reference optic so the expected results were well known. This test was intended mainly to insure proper operation of the VSHOT. In some cases rough prototype equipment was used since the final versions were not yet ready. For instance, a small, somewhat warped poster board was used as the target. A check of the laser scanner calibration indicated a good calibration with small errors present.

The test article was a 4" OD circular front surface Al mirror with 11.81 in (300 mm) focal length. A test pattern of 3.24" diameter was used, with 0.25 in spacing and grid randomization off, leading to 134 total

points. The optic was placed 42.5 inches from the target. This geometry is different from what the VSHOT was designed to test. The mirror is much smaller and close, and our analysis estimated a an uncertainty of ±0.002 to ±0.136 mrad (Table 1, case 1-2), depending upon the uncertainty in the measurement of Σ. Consequently, we expected that a second order fit with focal length of 11.81 inches would be found as the best fit. With that fit, random errors with RMS value between 0.002 and 0.136 mrad were expected. As will be seen, however, the results differed slightly from expectations.

Multiple fits of the data were performed, and Table 2 shows the results of the analysis. The focal length was found to be approximately 12.25 inches, a 3.7% error from the true focal length. Only one measurement of Σ was made. Treating this as a bias error in Σ means the random error is then only ±0.002 mrad as in case 1 of Table 1.

A second order fit is clearly adequate because higher order fits do not reduce the RMS error, which is within the estimated uncertainty bounds. Figure 5 shows the residuals plot, sometimes called a whisker plot, for fit A. It is clear the residuals are not random in nature, but are dominated by a clockwise rotation bias error of 0.265 mrad, caused by a rotation of 0.015 degrees in one of the subsystem calibrations. We suspect the grid of spots used in the video calibration was the cause. Since this is a very small rotation of the hardware, it is hard to prevent. We plan to implement a software correction instead. For typical solar concentrators, errors would exceed those from a rotation such as this. A tilt of a subsystem calibration causes the type of errors seen in Figure 5 because the measured locations are rotated from their true values.

The center test point and the two points just above and below have very large errors because their return rays were at least partially "lost" in the source spot hole. Considering the expected uncertainty and testing procedures were less rigorous than for a normal test, the results indicate the system worked properly.

Table 2. Results from the reference optic test

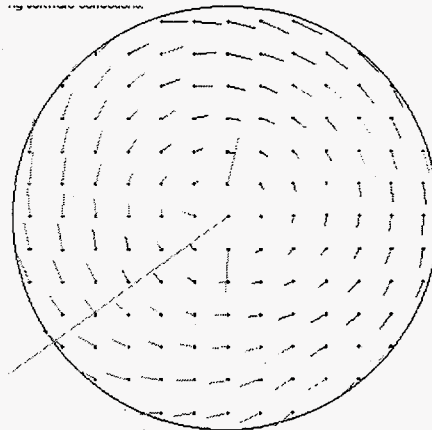| Fit	Fit Order	Est. f (in.)	f_x (in.)	f_y (in.)	RMS error (mrad)
A	2	11.8	12.28	12.21	.265
B	4	11.8	12.28	12.22	.261
C	6	11.8	12.27	12.21	.262
D	8	11.8	12.22	12.18	.261

Figure 5. Fit A residuals plot for reference optic

7.2 Test of a Windshield Sample

This test was performed to explore the use of the VSHOT in a non-solar applications. A small sample from the corner of a windshield was filled with a 4"x4" test pattern containing 156 points. The expected shape was unknown, so there was no way of gauging the accuracy of the final results in this test. The windshield was placed 38.0 inches from the target. The measurement uncertainty was not estimated, but should be similar to the previous test (4% bias in focal length, and ±0.002 mrad random error).

Table 3 lists the fitting results. Immediately apparent is the large difference in x and y focal lengths. This was expected due to the curvature of the windshield section tested. For this specimen, a fourth order fit appears to do a much better job approximating the surface shape than a second order fit as evidenced by the significant drop in RMS error. This higher order best fit is consistent with the more complex curvature

of the windshield section. Higher order fits seem to add little to the accuracy. In fit D an estimated focal length larger, as opposed to smaller, than calculated was used as a starting point for the fit. This had no effect on the results when compared with fit C. Figure 6 shows the residuals plot for fit B. Again the residuals appear rotated, this time 0.02 degrees counter-clockwise. This was also true for fits B-F, we believe for the same reasons as in the previous test.

Again, some points adjacent to the middle of the test article have very large errors because their return rays were at least partially "lost" in the source spot hole.

Table 3. Results from the windshield analysis

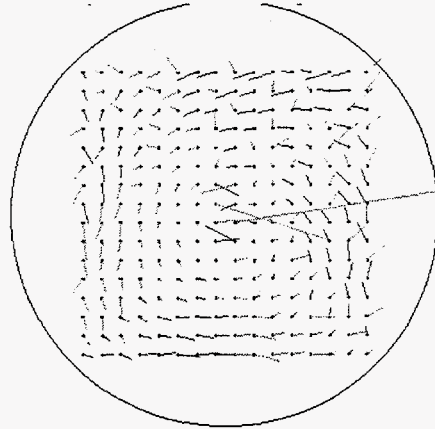| Fit	Fit Order	Est. f (in.)	f_x (in.)	f_y (in.)	RMS error (mrad)
A	2	10	34.6	62.7	.802
B	4	10	34.6	63.1	.377
C	6	10	34.7	63.0	.375
D	6	100	34.7	63.0	.375
E	8	10	34.8	64.0	.373
F	10	10	35.1	65.2	.371

Figure 6. Fit B residuals plot for windshield

8. CONCLUSIONS

The VSHOT is a flexible device capable of testing large reflectors with f/# greater than 0.45 and RMS optical error in the 0.1-10 milliradian range. It utilizes the scanning Hartmann approach that has been proven accurate. Measurement error may enter during subsystem calibrations or actual testing. Estimated, one-sigma, random measurement uncertainty is less than ± 0.05 mrad for typical solar reflectors and less than ±0.2 mrad for very small diameter, small f/#s. Experimental sensitivity studies are planned. A correction for movement of the apparent laser beam source will be implemented.

Preliminary results from a reference optic indicate proper operation of the VSHOT. A windshield segment was also tested, demonstrating the viability of testing non-solar reflectors. The slope error plot of both articles indicates that a very slight rotation of one of the subsystem calibrations was present. A software correction is needed to eliminate this error.

9. ACKNOWLEDGEMENTS

10. REFERENCES

1. T.J. Wendelin, G.J. Jorgensen, R.L. Wood, "SHOT: A method for Characterizing the Surface Figure and Optical Performance of Point Focus Solar Concentrators," *Solar Engineering 1991*, p.555-560, American Society of Mechanical Engineers, New York, 1991

2. J.W. Grossman, "Development of a 2*f* Optical Performance Measurement System," *Solar Engineering 1994*, p.25-32, American Society of Mechanical Engineers, New York,1994

3. J.W. Grossman, R.M. Edgar, "Transforming the Sandia 2*f* Optical Performance Measurement System to Color," *Solar Engineering 1996*, p.105-112, American Society of Mechanical Engineers, New York, 1996

4. T.J. Wendelin, J.W. Grossman, "Comparison of Three Methods for Optical Characterization of Point-Focus Concentrators," *Solar Engineering: 1995- Volume 2*, p.775-780, American Society of Mechanical Engineers, New York, 1995

5. Malacara, D., (1978). *Optical Shop Testing*. John Wiley and Sons, New York.

6. G. Jorgensen., T. Wendelin, M. Carasso, "Determination of Accuracy of Measurements by NREL's Scanning Hartmann Optical Test Instrument," NREL Technical Report #TP-257-4190, April 1991.